Geophysical Research Letters

RESEARCH LETTER
10.1029/2024GL111364

Baffin Bay Ice Export and Production From Sentinel-1, the RADARSAT Constellation Mission, and CryoSat-2: 2016–2022

S. E. L. Howell[1], D. G. Babb[2], J. C. Landy[3], G. W. K. Moore[4,5], T. J. Ballinger[6], K. McNeil[4], B. Montpetit[1], and M. Brady[1]

[1]Climate Research Division, Environment and Climate Change Canada, Toronto, ON, Canada, [2]Centre for Earth Observation Science, University of Manitoba, Winnipeg, MB, Canada, [3]Department of Physics and Technology, The Arctic University of Norway, Tromsø, Norway, [4]Department of Physics, University of Toronto, Toronto, ON, Canada, [5]Department of Chemical and Physical Sciences, University of Toronto Mississauga, Mississauga, ON, Canada, [6]International Arctic Research Center, University of Alaska Fairbanks, Fairbanks, AK, USA

Key Points:

- High quality and consistent satellite derived estimates are provided for Baffin Bay sea ice export
- Approximately 80% of the Baffin Bay ice exported via Davis Strait is locally produced
- Annual sea ice export from Baffin Bay represents ~59% of the volume flux and ~111% of the area flux compared to Fram Strait

Correspondence to:
S. E. L. Howell,
Stephen.Howell@ec.gc.ca

Citation:
Howell, S. E. L., Babb, D. G., Landy, J. C., Moore, G. W. K., Ballinger, T. J., McNeil, K., et al. (2024). Baffin Bay ice export and production from Sentinel-1, the RADARSAT Constellation Mission, and CryoSat-2: 2016–2022. *Geophysical Research Letters*, *51*, e2024GL111364. https://doi.org/10.1029/2024GL111364

Received 15 JUL 2024
Accepted 3 NOV 2024

Abstract Baffin Bay is located between Greenland and several islands of the Canadian Arctic, providing a conduit for the downstream transport of ice and freshwater to the North Atlantic via Davis Strait. Using satellite observations from Sentinel-1, the RADARSAT Constellation Mission, and CryoSat-2, we estimated the sea ice export through Davis Strait and winter ice production in Baffin Bay from 2016 to 2022. The average annual ice export for this 6-year period was 981 ± 193 × 10^3 km^2 for area 816 ± 130 km^3 for volume, and 653 ± 130 km^3 for solid freshwater, all of which are considerably higher than previously reported estimates. The average winter ice area production upstream of Davis Strait was 758 × 10^3 km^2 and the volume production was 589 km^3 indicating that more than 80% of the ice exported out of Baffin Bay was produced locally. Compared to Fram Strait, sea ice fluxes through Davis Strait represent ~59% of the volume and ~111% of the area.

Plain Language Summary Baffin Bay is located between Greenland and several islands of the Canadian Arctic. Sea ice and freshwater is transported downstream to the North Atlantic through Davis Strait located at the southern end of Baffin Bay. Using the latest state-of-the-art satellite observations we estimated the amount of sea ice and freshwater transported through Davis Strait in addition to the amount of ice produced in Baffin Bay from 2016 to 2022. Our ice transport and ice production estimates were considerably higher than previously reported estimates. Sea ice transport from Davis Strait represented 111% of area and 59% of the volume of the Fram Strait which is the Arctic's major ice export passageway.

1. Introduction

Baffin Bay is located between Greenland and several islands of the Canadian Arctic (Ellesmere Island, Devon Island, and Baffin Island; Figure 1). The ice cover is predominantly seasonal ice that forms within Baffin Bay, though a small portion of multi-year sea ice (MYI) is imported from the Arctic Ocean via Nares Strait and the Canadian Arctic Archipelago (CAA) via Lancaster Sound (Agnew et al., 2008; Kwok et al., 2010; Melling, 2002; Moore et al., 2021). Sea ice area within Baffin Bay from June to October has decreased by 17.5%/decade over the period of 1968–2023 with a sustained decrease since ~2001 (Figure 1). Previous studies have also observed large decreases in Baffin Bay sea ice area (Ballinger et al., 2022; Moore, 2006; Tivy et al., 2011).

A persistent trough between Greenland and Baffin Island drives southerly winds that transports the ice southwards and advects sea ice through Davis Strait at the southern end of the Baffin Bay toward the North Atlantic (Agnew et al., 2008; Kwok, 2007; Wilson et al., 2001) and also contributes to the formation and persistence of the North Water (NOW) Polynya at the northern end of the Baffin Bay (Dunbar & Dunbar, 1972). Sea ice export through Davis Strait presents downstream marine hazards to offshore development and navigation along the East Coast of Canada (Barber et al., 2018) and represents a key freshwater flux in the larger freshwater budget of the North Atlantic which impacts the Atlantic meridional overturning circulation (Aagaard & Carmack, 1989; Carmack et al., 2016; Gregory et al., 2005; Jahn et al., 2010). Previous studies have estimated the annual sea ice area export to be between ~394–585 × 10^3 km^2 (Bi et al., 2019; Kwok, 2007; Liang et al., 2021) and the annual sea ice volume export between ~400 and 800 km^3 through Davis Strait (Curry et al., 2014; Kwok, 2007). The

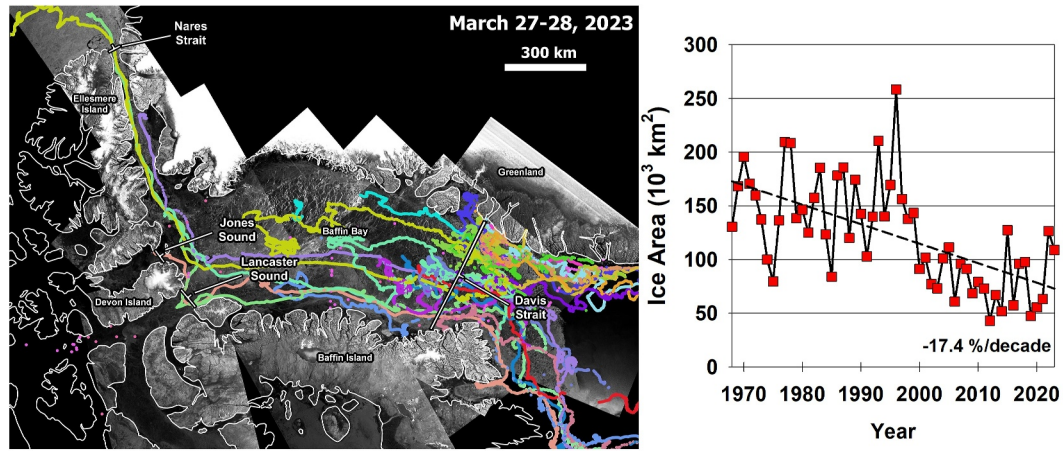

Figure 1. Map of the Baffin Bay study region with the location of the sea ice export gate (Davis Strait), import gates (Nares Strait, Jones Sound, and Lancaster Sound), and buoy trajectories (left). Time series of the average June to October sea ice area in Baffin Bay from 1968 to 2023 (right). Background for the left panel is RCM imagery on March 27–28, 2023 (RCM © Government of Canada). Data for the right panel is from the Canadian Ice Service.

annual sea ice freshwater flux relative to 38.4 psu through Davis Strait to the North Atlantic has been estimated to be between 320 and 788 km^3 (Azetsu-Scott et al., 2012; Curry et al., 2011, 2014).

A wide range of data sources and techniques have been utilized to provide the aforementioned observed estimates. For example, Kwok (2007) used 12.5 km resolution Advanced Microwave Scanning Radiometer (AMSR-E) data to derive ice concentration and motion to estimate the sea ice area flux at Davis Strait for 2002–2007. Bi et al. (2019) and Liang et al. (2021) used 25 km sea ice motion and ice concentration from the National Snow and Ice Data Center (NSIDC) (Comiso, 2023; Tschudi et al., 2020) to provide area ice area flux estimates from 1979 to 2017. Curry et al. (2015) used AMSR-E sea ice motion and ice concentration together with a moored sensor array to estimate ice volume and freshwater flux from 2004 to 2010. Azetsu-Scott et al. (2012) used the oxygen isotope composition ($\delta^{18}O$) to estimate the volume freshwater flux across Davis Strait for 2010–2011. These approaches are limited in time and space and when combined with disparate data sources, uncertainty can be exacerbated. The recent availability of consistent high spatiotemporal resolution synthetic aperture radar (SAR) imagery from Sentinel-1 and the RADARSAT Constellation Mission (RCM) together with CryoSat-2 data provide a unique opportunity to revisit the area and volume flux of ice in and out of Baffin Bay by providing year-round high-quality estimates.

In this study, we make use of observations from Sentinel-1, the RCM, and CryoSat-2 to estimate and discuss the recent sea ice area and volume flux variability of Baffin Bay from 2016 to 2022. We also make use of coincident sea ice area and ice volume flux estimates through the adjoining passageways of Nares Strait, Jones Sound, and Lancaster Sound to estimate winter ice production in Baffin Bay. Finally, we compare the total downstream ice and equivalent solid freshwater flux to the North Atlantic through Davis Strait to Fram Strait.

2. Data and Methods

SAR imagery at HH polarization from Sentintel-1 and RCM together with year-round sea ice thickness estimates from the CryoSat-2 radar altimeter were the primary data sources used in this analysis. SAR imagery was resampled to 200 m and was available with ∼1-day temporal resolution from October 2016 to September 2022. RCM imagery is available online at Natural Resources Canada's Earth Observation Data Management System (https://www.eodms-sgdot.nrcan-rncan.gc.ca). Sentinel-1 imagery is available at the Copernicus Open Access Hub (https://scihub.copernicus.eu/dhus/#/home). CryoSat-2 ice thickness estimates were available continuously on a biweekly time interval from October 2016 to July 2022 at https://data.bas.ac.uk/full-record.php?id=GB/NERC/BAS/PDC/01613, derived with the method described in Landy et al. (2022).

Supporting data used in this analysis included weekly sea ice concentration with a spatial resolution of ~1 km from the Canadian Ice Service (CIS) digital ice charts available at https://iceweb1.cis.ec.gc.ca/Archive/page1.xhtml?lang=en. The weekly CIS ice charts integrate all available sea ice information from various sources with the primary source being synthetic SAR and the reader is referred to Tivy et al. (2011) for a complete description. We also used Monthly sea level pressure (SLP) and 10 m wind speed from ERA5 (Copernicus Climate Change Service(C3S), 2017) available at https://cds.climate.copernicus.eu/cdsapp#!/home and previous ice area and volume flux estimates from Nares Strait (Howell et al., 2023) and Lancaster Sound (Howell, Babb, Landy, Glissenaar, et al., 2024).

The sea ice area flux at the Davis Strait gate (460 km aperture) located at the southern end of Baffin Bay was estimated from October 2016 to September 2022 (Figure 1). Although previous studies have indicated gate location could potentially impact the long-term trend in sea ice area flux (i.e., Bi et al., 2019; Liang et al., 2021), we selected our gate location analogous to Kwok (2007) who found that sea ice area flux is comparable between gates placed at the south end of Baffin Bay compared to the north. Our approach is based on previous work that uses sequential pairs of SAR imagery to derive sea ice area and volume fluxes (e.g., Howell et al., 2013; Howell et al., 2023; Howell, Babb, Landy, Glissenaar, et al., 2024; Kwok, 2007; Moore et al., 2021). First, sea ice motion is determined for each sequential SAR image pair at 200 m spatial resolution using the Environment and Climate Change Canada Automated Sea Ice Tracking System (ECCC-ASITS; Howell et al., 2022) that is based on the Komarov and Barber (2014) feature tracking algorithm. All sea ice motion vectors at 200 m spatial resolution are then interpolated to a 30 km buffer region around the Davis Strait gate. Sea ice motion and ice concentration from the Canadian Ice Service ice charts are then sampled at 5 km intervals along the gate using the following equation:

$$F_A = \sum c_i u_i \Delta x \tag{1}$$

where, Δx is the spacing along each gate (i.e., 5 km), u_i is the ice motion normal to the flux gate at the ith location and c_i is the sea ice concentration determined from the Canadian Ice Service ice charts. The sea ice area flux values for each sequential pair of SAR imagery from Equation 1 are summed over each month from October 2016 to September 2022. Positive flux values represent export from Baffin Bay via Davis Strait and negative values represent ice import into Baffin Bay via Davis Strait.

The uncertainty (σ_{FA}) in F_A can be estimated following Kwok and Rothrock (1999) by assuming negligible uncertainty in CIS ice chart ice concentration which have no reliable uncertainty estimate and that errors in sea ice motion are additive, uncorrelated, and normally distributed using the following equation:

$$\sigma_{FA} = \frac{\sigma_u L}{\sqrt{N_s}} \tag{2}$$

where, σ_u is the error in SAR derived ice motion, L is the width of the gate, and N_s is the number of samples across the gate. We estimate the value of σ_u to be 1.41 km based on comparison between SAR and buoy u and v displacements from the International Arctic Buoy Program (IABP; https://iabp.apl.uw.edu/data.html) for the 30 km buffer surrounding the Davis Strait gate during the winter and melt season (Figure 1; Figure 2a). The ice area flux uncertainty on a monthly basis (σ_T) can subsequently be estimated using the following equation:

$$\sigma_T = \sigma_{FA}\sqrt{N_D} \tag{3}$$

where, N_D is the number of observations per month (~30) and the daily errors are also assumed to be uncorrelated. Solving for Equations 1 and 2 we estimate the uncertainty in the monthly sea ice area flux at Davis Strait to be 366 km^2 and the annual uncertainty to be ~4 × 10^3 km^2, or less than 0.5% of the total annual sea ice area flux.

The sea ice volume flux from Baffin Bay via Davis Strait was determined from the product of the monthly ice area flux and the monthly average CryoSat-2 sea ice thickness within the 200 km buffer around each gate. We use the larger (i.e., 200 km) buffer for volume flux given the coarse spatial resolution of the thickness product (i.e., 80 km). We estimate the uncertainty (σ_{FV}) in the ice volume flux following Kwok and Rothrock (1999) using:

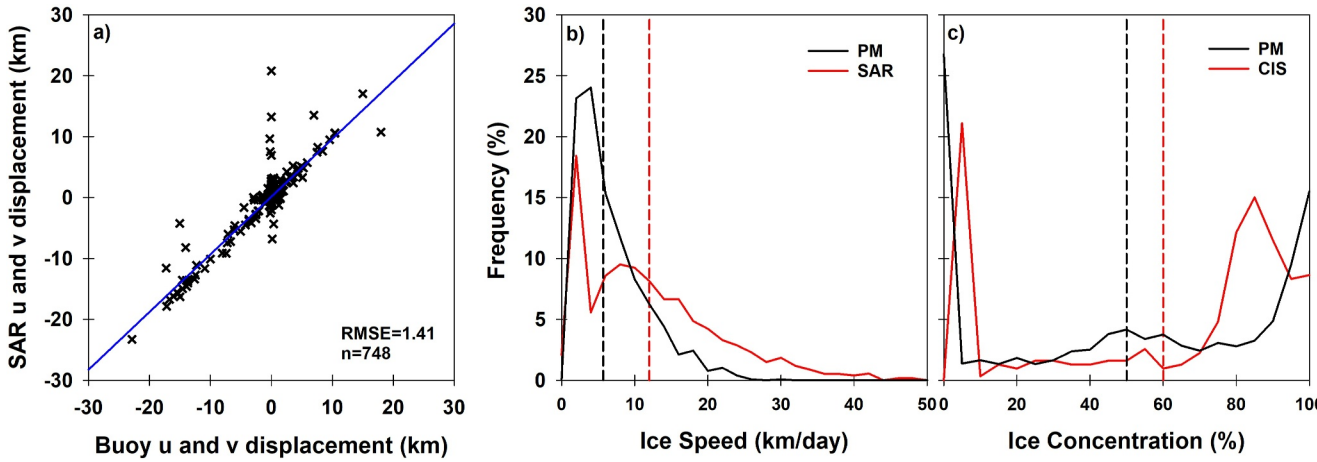

Figure 2. (a) Comparison between ice motion vectors derived by the Komarov and Barber (2014) automated sea ice tracking algorithm from Sentinel-1 and RCM SAR images with buoy data in the vicinity of Davis Strait. (b) Frequency distribution (%) of ice speed from Sentinel-1 and RCM sea ice motion data at 200 m spatial resolution and the NSIDC passive microwave sea ice motion data at 25 km spatial resolution in the 30 km buffer region of the Davis Strait flux gate. (c) Frequency distribution (%) of sea ice concentration from CIS ice charts and passive microwave observations (Comiso and Gersten, 2023) in the 30 km buffer region of the Davis Strait flux gate. The dashed vertical lines indicate the 2016–2022 mean.

$$\sigma_{FV} = \sqrt{(F_A\sigma_h)^2 + (h\sigma_T)^2} \quad (4)$$

where, h is the ice thickness and σ_h is the uncertainty in thickness. σ_h for the outer gates is taken from Landy et al. (2022). Solving for Equation 4 we estimate the monthly uncertainty in the ice volume flux at Davis Strait to be 26 km^3 and an annual uncertainty of 311 km^3, or ~38% of the total annual sea ice volume flux.

3. Results and Discussion

3.1. Baffin Bay Ice Area and Volume Export

The interannual variability of the average monthly ice area and volume fluxes through Davis Strait is high (Figure 3). The average monthly sea ice area flux was $82 \pm 86 \times 10^3$ km^2 with a maximum of 297×10^3 km^2 reached in March 2020 (Figure 3a). For volume flux, the average monthly value was 70 ± 81 km^3 with a maximum of 262 km^3 also in March of 2020 (Figure 3c). A distinct annual cycle is apparent for both the ice area and volume fluxes, with export peaking in March and being negligible from August to October when Davis Strait is ice-free (Figure 3). This pattern is associated with the seasonal growth and melt of sea ice upstream of Davis Strait in Baffin Bay together with the annual cycle in the SLP gradient across Davis Strait that dictates winds and therefore ice motion through Davis Strait (Kwok, 2007). Overall, there is a moderately strong relationship between the Davis Strait cross-gate pressure gradient (ΔP) and the ice area and volume fluxes for all months ($n = 72$) with statistically significant ($p < 0.05$) correlation coefficients of 0.69 and 0.52, respectively (Figure 3), which is in agreement with Liang et al. (2021).

Over the 6-year period, an annual average of 981×10^3 km^2 of ice area and 816 km^3 of ice volume was exported through Davis Strait. Previous studies typically only examine the winter ice flux from November to May, and hence to compare our estimates we first determine the average area and volume ice fluxes from November to May that are 915×10^3 km^2 and 764 km^3, respectively. This is considerably higher than the average ice area fluxes of 584×10^3 km^2 reported by Liang et al. (2021) for the period from 1979 to 2017, 530×10^3 km^2 reported by Kwok (2007) for the period from 2002 to 2007 and 585×10^3 km^2 reported by Curry et al. (2014) for the period from 2004 to 2010. Similarly, our estimate of volume export is nearly double the previous estimate of 407 km^3 reported by Curry et al. (2014) for the period from 2004 to 2010.

The differences between our ice flux estimates and previous studies are the result of a combination of factors including geographic definitions of ice exchange gate locations and technical sea ice motion algorithm differences but the source data is the most influential. Specifically, passive microwave observations underestimate the ice

10.1029/2024GL111364

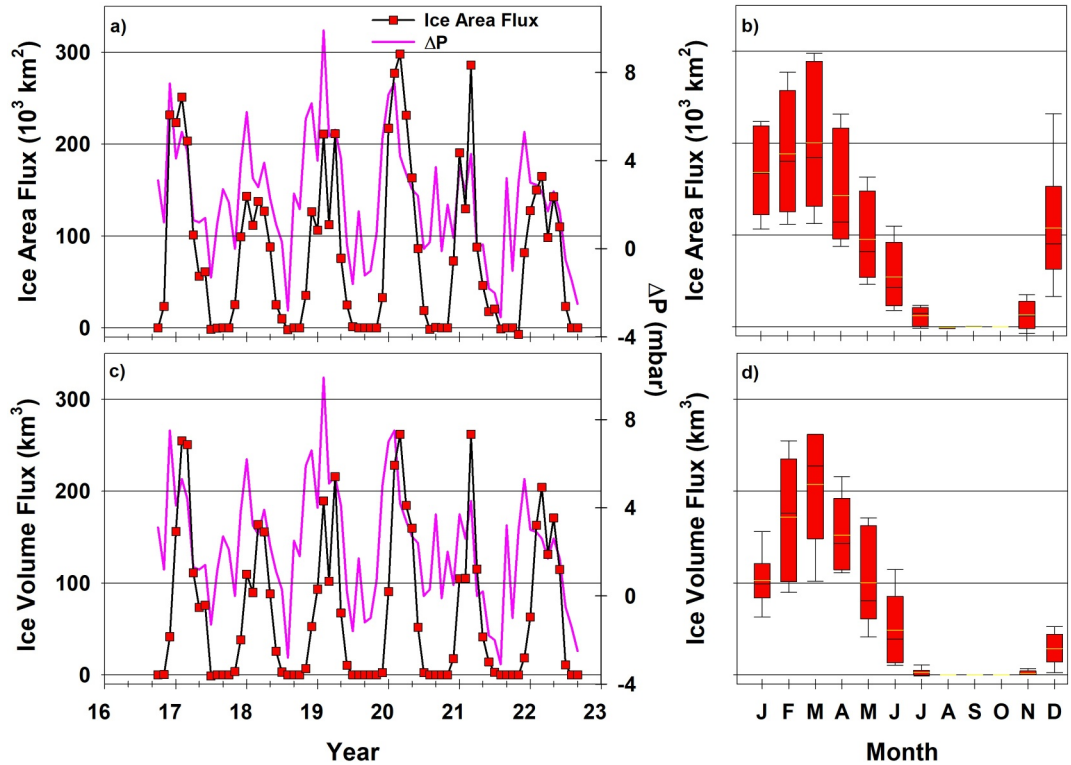

Figure 3. (a) Time series of monthly ice area flux at Davis Strait together with Davis Strait cross-gate pressure gradient (ΔP) from October 2016 to September 2022, (b) box plots of mean month monthly sea ice area flux from January to December at Davis Strait, (c) time series of monthly ice volume flux at Davis Strait together with Davis Strait cross-gate pressure gradient (ΔP) from October 2016 to September 2022, and (d) box plots of mean month monthly sea ice volume flux from January to December at Davis Strait.

motion at the fastest drift speeds as spatial aliasing and temporal decorrelation occur more easily when using kilometer scale spatial resolution (6–25 km) observations compared to meter scale (i.e. 200 m) SAR observations (Bi et al., 2019; Howell et al., 2022; Kwok et al., 1998; Lavergne et al., 2010). Figure 2b illustrates that mean ice speed from the SAR imagery was 12 km/day, more than double the mean ice speed of 5.7 km/day from passive microwave observations and indicates that SAR imagery captures more of the true ice drift variability especially, fast small-scale ice motion above the mean. In addition, the CIS ice concentration is more representative than passive microwave estimates that can considerably underestimate sea ice concentration especially during the shoulder seasons (Agnew & Howell, 2003). Figure 2c illustrates that although comparable, the CIS ice charts provide higher concentration values than passive microwave with means of 60% and 50%, respectively. If we just utilize passive microwave observations the 6-year winter average ice area flux through Davis Strait is about 523×10^3 km^2, which is just more than half the amount determined from SAR and the CIS ice charts.

3.2. Winter Ice Production Within Baffin Bay

Over the 6-year period, the average winter (November to May) ice area fluxes from Lancaster Sound and Nares Strait were 99×10^3 km^2 and 48×10^3 km^2, or ~11% and ~5% of the Davis Strait ice area flux (Figure 4a). With respect to average winter ice volume, Lancaster Sound imported 52 km^3 or 7% of the Davis Strait volume flux and Nares Strait imported 92 km^3 or ~12% of the Davis Strait volume flux (Figure 4b). The larger volume flux contribution from Nares Strait than Lancaster Sound, despite the similar area flux, is driven by the reservoir of thick MYI located north of Nares Strait in the Lincoln Sea (Landy et al., 2022). Jones Sound provided negligible ice area and volume flux contributions but was still included in the ice production estimates (Figure 4).

Subtracting the winter average Davis Strait sea ice export from the winter average sea ice import at Lancaster Sound, Jones Sound, and Nares Strait, we estimate the winter ice area production within this bounded region to be 763×10^3 km^2 and the volume production is 619 km^3. This suggests that more than 80% of the ice being exported

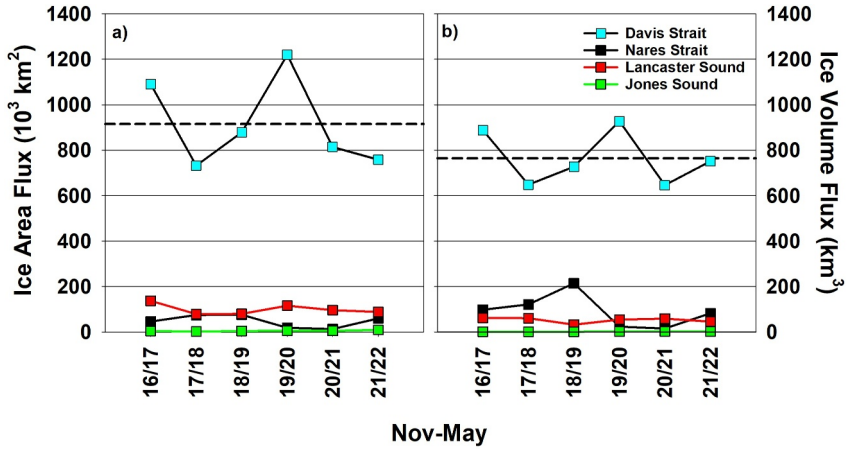

Figure 4. Time series of the winter (November to May) ice area (a) and volume (b) fluxes at Davis Strait, Nares Strait, Lancaster Sound, and Jones Sound from 2016 to 2022. The dashed horizontal black line indicates the Davis Strait 2016–2022 ice flux mean.

out of Baffin Bay via Davis Strait during the winter has been produced locally. Approximately one third of this locally sourced ice can be attributed to ice production specifically in the NOW from previous studies which has been estimated annually to range from 144 to 186 km^3 for volume (Iwamoto et al., 2014; Ren et al., 2022) and 280–300 × 10^3 km^2 for area (Bi et al., 2019; Kwok, 2007).

Based on the amount of ice produced upstream of the Davis Strait flux gate together with the relationship between ice area flux and SLP (Figure 2a) we suggest variability in the ice export at Davis Strait is influenced more by local atmosphere and ocean processes rather than import contributions from Nares Strait, Lancaster Sound, or Jones Sound. Indeed, the ice arches that develop in Nares Strait and Lancaster Sound have exhibited long-term declines in duration since the late 1970s, which increases the overall ice flux through Baffin Bay (Moore et al., 2021; Vincent, 2019, 2023). Nares Strait, has experienced anomalous formation and collapse of its ice arches in recent years (Moore et al., 2021; Moore & McNeil, 2018). However, we find no association between years of high ice import from Lancaster Sound or Nares Strait to export at Davis Strait. Specifically, the year of lowest import (2019–2020) from Nares Strait and Lancaster Sound corresponds to the largest ice area flux at Davis Strait (Figure 4a). Moreover, the year of largest ice volume import from Nares Strait (2018–2019) only had the fourth largest volume export from Davis Strait (Figure 4b).

3.3. Comparison With Fram Strait and Downstream Contribution to the North Atlantic

Quantifying ice flux through Davis Strait is of particular importance as it is one of only four terms that dictate the transport of freshwater from the Arctic Ocean to the North Atlantic where it influences the global thermohaline circulation (Jahn et al., 2010). The four terms are the liquid and solid freshwater fluxes through Davis Strait and Fram Strait, which given that all of the sea ice melts after drifting south through these straits, sum to provide a total liquid freshwater flux to the North Atlantic. It is therefore useful to compare our estimates to that of Fram Strait.

Our annual average sea ice area flux through Davis Strait of 981 × 10^3 km^2 is ∼11% greater than the long-term annual average of 880 × 10^3 km^2 reported by Smedsrud et al. (2017) for Fram Strait. This is a considerable contrast compared to previous studies who reported the annual ice area flux at Davis Strait to be less than Fram Strait (Bi et al., 2019; Kwok, 2007). Moreover, the long-term estimate from Smedsrud et al. (2017) were partially based on SAR derived 3-day ice motion rather than coarse passive microwave products that are known to underestimate ice drift speeds and therefore ice export. Further comparison between the two straits with consistent approaches is warranted as interannual variability is high between the two gates together with the recent (i.e., 1979 to present) positive trend in ice area flux through Davis Strait (Bi et al., 2019) and Fram Strait (Smedsrud et al., 2017).

In terms of sea ice volume export, Sumata et al. (2022) reported that the annual volume flux through Fram Strait from 1990 to 1999 was 2450 km^3, declined to 1760 km^3 from 2000 to 2009, and then further to 1390 km^3 from

2010 to 2017. There was also an anomalous drop in 2018, however, for a more conservative comparison we just consider the 2010–2017 average value. Our 6-year annual average volume flux from Davis Strait is 816 km^3 which represents 59% of the 2010–2017 annual average Fram Strait volume flux and is greater than the 30%–33% previously estimated by Kwok (2007) and Curry et al. (2014). The difference in these proportions reflects a combination of differences in methods and data sources together with the long-term reduction in sea ice volume export through Fram Strait reported by Sumata et al. (2022). The reduction between volume fraction of the sea ice flux through Davis Strait compared to Fram Strait is caused by the difference in ice types and therefore ice thickness. Specifically, seasonal ice that primarily formed within Baffin Bay is exported through Davis Strait, whereas thicker seasonal ice and MYI from the Central Arctic are exported through Fram Strait (Babb et al., 2023; Sumata et al., 2023).

To convert estimates of sea ice volume flux to liquid freshwater fluxes, relative to a salinity of 34.8, we scale them by 0.8 (Spreen et al., 2020). From this we estimate an annual average solid freshwater flux of 653 km^3 through Davis Strait with an uncertainty of 249 km^3. The value of 653 km^3 is more than double the value compiled in the review of Haine et al. (2015) of 320 km^3 and larger than the annual land ice freshwater flux contribution through Davis Strait of between 514 and 563 km^3 reported by Bamber et al. (2018).

4. Conclusions

We estimated sea ice export and winter ice production from Sentinel-1, RCM, and CryoSat-2 in Baffin Bay over the period of 2016–2022. Over the 6-year period, an annual average of 981×10^3 km^2 of ice area and 816 km^3 of ice volume was exported out of Baffin Bay via Davis Strait. The average annual solid freshwater flux to the North Atlantic from Davis Strait was 653 km^3. Our values were considerably higher than previous studies which we attribute primarily to result of an ice speed bias from passive microwave sea ice motion. As a result, we find that average annual sea ice area and volume fluxes at Davis Strait have been considerably higher relative to Fram Strait than previously reported by at 111% and 59%, respectively. Our estimates are therefore more representative of the current amount of ice being transported southward to the North Atlantic via Davis Strait which has important implications for understanding the current state of freshwater fluxes and the freshwater budget of the Arctic Ocean.

We also found that from 2016 to 2022, more than 80% of the ice exported out of Baffin Bay via Davis Strait during the winter months was produced locally. Despite Baffin Bay recently experiencing dramatic reductions in sea ice during the summer and autumn months, it appears as though ice production during the winter months is still robust. We found no evidence of significant changes or negative anomalies in Baffin Bay ice export over our 6-year study period, or a significant decline compared to estimates from the 2000s. Sea ice fluxes from Nares Strait, Lancaster Sound, and Jones Sound did not exert appreciable influence on the flux of ice downstream at Davis Strait. Further, we found no association between years of high ice import from Lancaster Sound or Nares Strait to export at Davis Strait despite the recent increase in the Nares Strait ice flux together with reduced ice arch duration at both Lancaster Sound and Nares Strait. This suggests that much larger changes in upstream ice flux magnitudes would likely be required to significantly impact ice export at Davis Strait.

Data Availability Statement

The year-round sea ice thickness observations from CryoSat-2 (J. Landy & Dawson, 2022) are available via the Polar Data Centre. The monthly sea ice area and volume flux values from October 2016 to September 2022 (Howell, Babb, Landy, Moore, et al., 2024) are available on Environment and Climate Change Canada's (ECCC) Open Data Server.

Acknowledgments
DB is supported by the Canada Excellence Research Chair program (D. Dahl-Jensen). JL acknowledges support from the Research Council of Norway (RCN) for the INTERAAC project (#328957) and the DynAMIC project (#343069) and from the European Research Council for the SI/3D project (#101077496). GWKM would like to acknowledge support from the Natural Sciences and Engineering Research Council of Canada.

References

Aagaard, K., & Carmack, E. C. (1989). The role of sea ice and other fresh water in the Arctic circulation. *Journal of Geophysical Research*, *94*(C10), 14485–14498. https://doi.org/10.1029/JC094iC10p14485

Agnew, T., & Howell, S. (2003). The use of operational ice charts for evaluating passive microwave ice concentration data. *Atmosphere-Ocean*, *41*(4), 317–331. https://doi.org/10.3137/ao.410405

Agnew, T., Lambe, A., & Long, D. (2008). Estimating sea ice area flux across the Canadian Arctic Archipelago using enhanced AMSR-E. *Journal of Geophysical Research*, *113*(C10), 2007JC004582. https://doi.org/10.1029/2007JC004582

Azetsu-Scott, K., Petrie, B., Yeats, P., & Lee, C. (2012). Composition and fluxes of freshwater through Davis Strait using multiple chemical tracers. *Journal of Geophysical Research*, *117*(C12), 2012JC008172. https://doi.org/10.1029/2012JC008172

Babb, D. G., Galley, R. J., Kirillov, S., Landy, J. C., Howell, S. E. L., Stroeve, J. C., et al. (2023). The stepwise reduction of multiyear Sea Ice area in the Arctic Ocean since 1980. *JGR Oceans*, *128*(10), e2023JC020157. https://doi.org/10.1029/2023JC020157

Ballinger, T. J., Moore, G. W. K., Garcia-Quintana, Y., Myers, P. G., Imrit, A. A., Topál, D., & Meier, W. N. (2022). Abrupt northern Baffin Bay autumn warming and Sea-ice loss since the turn of the twenty-first century. *Geophysical Research Letters*, *49*(21), e2022GL101472. https://doi.org/10.1029/2022GL101472

Bamber, J. L., Tedstone, A. J., King, M. D., Howat, I. M., Enderlin, E. M., van den Broeke, M. R., & Noel, B. (2018). Land ice freshwater budget of the Arctic and North Atlantic oceans: 1. Data, methods, and results. *Journal of Geophysical Research: Oceans*, *123*(3), 1827–1837. https://doi.org/10.1002/2017JC013605

Barber, D. G., Babb, D. G., Ehn, J. K., Chan, W., Matthes, L., Dalman, L. A., et al. (2018). Increasing mobility of high Arctic Sea Ice increases marine hazards off the East Coast of Newfoundland. *Geophysical Research Letters*, *45*(5), 2370–2379. https://doi.org/10.1002/2017GL076587

Bi, H., Zhang, Z., Wang, Y., Xu, X., Liang, Y., Huang, J., et al. (2019). Baffin Bay sea ice inflow and outflow: 1978–1979 to 2016–2017. *The Cryosphere*, *13*(3), 1025–1042. https://doi.org/10.5194/tc-13-1025-2019

Carmack, E. C., Yamamoto-Kawai, M., Haine, T. W. N., Bacon, S., Bluhm, B. A., Lique, C., et al. (2016). Freshwater and its role in the Arctic Marine System: Sources, disposition, storage, export, and physical and biogeochemical consequences in the Arctic and global oceans. *JGR Biogeosciences*, *121*(3), 675–717. https://doi.org/10.1002/2015JG003140

Comiso, J. C. (2023). Bootstrap Sea ice concentrations from Nimbus-7 SMMR and DMSP SSM/I-SSMIS. (NSIDC-0079, version 4) [Dataset]. *Boulder, Colorado USA. NASA National Snow and Ice Data Center Distributed Active Archive Center*. [describe subset used if applicable]. https://doi.org/10.5067/X5LG68MH013O 11 07 2024.

Comiso, J. C., & Gersten, R. A. (2023). Bootstrap Sea ice concentrations from Nimbus-7 SMMR and DMSP SSM/I-SSMIS, version 4. https://doi.org/10.5067/X5LG68MH013O

Copernicus Climate Change Service (C3S). (2017). ERA5: Fifth generation of ECMWF atmospheric reanalyses of the global climate. *Copernicus Climate Change Service Climate Data Store (CDS)*. Retrieved from https://cds.climate.copernicus.eu/cdsapp#!/home

Curry, B., Lee, C. M., & Petrie, B. (2011). Volume, freshwater, and heat fluxes through Davis Strait, 2004–05. *Journal of Physical Oceanography*, *41*(3), 429–436. https://doi.org/10.1175/2010JPO4536.1

Curry, B., Lee, C. M., Petrie, B., Moritz, R. E., & Kwok, R. (2014). Multiyear volume, liquid freshwater, and Sea Ice transports through Davis Strait, 2004–10. *Journal of Physical Oceanography*, *44*(4), 1244–1266. https://doi.org/10.1175/JPO-D-13-0177.1

Dunbar, M., & Dunbar, M. J. (1972). 21.—The history of the North Water. *Proc. Sect. B. Biol.*, *72*(1), 231–241. https://doi.org/10.1017/S0080455X00001788

Gregory, J. M., Dixon, K. W., Stouffer, R. J., Weaver, A. J., Driesschaert, E., Eby, M., et al. (2005). A model intercomparison of changes in the Atlantic thermohaline circulation in response to increasing atmospheric CO 2 concentration. *Geophysical Research Letters*, *32*(12), 2005GL023209. https://doi.org/10.1029/2005GL023209

Haine, T. W. N., Curry, B., Gerdes, R., Hansen, E., Karcher, M., Lee, C., et al. (2015). Arctic freshwater export: Status, mechanisms, and prospects. *Global and Planetary Change*, *125*, 13–35. https://doi.org/10.1016/j.gloplacha.2014.11.013

Howell, S. E. L., Babb, D. G., Landy, J. C., Glissenaar, I. A., McNeil, K., Montpetit, B., & Brady, M. (2024). Sea ice transport and replenishment across and within the Canadian Arctic Archipelago, 2016–2022. *The Cryosphere*, *18*(5), 2321–2333. https://doi.org/10.5194/tc-18-2321-2024

Howell, S. E. L., Babb, D. G., Landy, J. C., Moore, G. W. K., Montpetit, B., & Brady, M. (2023). A comparison of Arctic Ocean Sea Ice export between Nares Strait and the Canadian Arctic Archipelago. *JGR Oceans*, *128*(4), e2023JC019687. https://doi.org/10.1029/2023JC019687

Howell, S. E. L., Babb, D. G., Landy, J. C., Moore, G. W. K., Montpetit, B., & Brady, M. (2024). Monthly sea ice area and volume flux values for Davis Strait, Nares Strait, Lancaster Sound, and Jones Sound from October 2016 to September 2022 [Dataset]. *Environment and Climate Change Canada's (ECCC) Open Data Server*. Retrieved from https://crd-data-donnees-rdc.ec.gc.ca/CPS/products/IceFlux/Publications/BaffinBay-Fluxes-GRL-2024.xlsx

Howell, S. E. L., Brady, M., & Komarov, A. S. (2022). Generating large-scale sea ice motion from Sentinel-1 and the RADARSAT Constellation Mission using the Environment and Climate Change Canada automated sea ice tracking system. *The Cryosphere*, *16*(3), 1125–1139. https://doi.org/10.5194/tc-16-1125-2022

Howell, S. E. L., Wohlleben, T., Dabboor, M., Derksen, C., Komarov, A., & Pizzolato, L. (2013). Recent changes in the exchange of sea ice between the Arctic Ocean and the Canadian Arctic Archipelago: Changes in Arctic Ocean-CAA ice exchange. *Journal of Geophysical Research: Oceans*, *118*(7), 3595–3607. https://doi.org/10.1002/jgrc.20265

Iwamoto, K., Ohshima, K. I., & Tamura, T. (2014). Improved mapping of sea ice production in the Arctic Ocean using AMSR-E thin ice thickness algorithm. *JGR Oceans*, *119*(6), 3574–3594. https://doi.org/10.1002/2013JC009749

Jahn, A., Tremblay, B., Mysak, L. A., & Newton, R. (2010). Effect of the large-scale atmospheric circulation on the variability of the Arctic Ocean freshwater export. *Climate Dynamics*, *34*(2–3), 201–222. https://doi.org/10.1007/s00382-009-0558-z

Komarov, A. S., & Barber, D. G. (2014). Sea ice motion tracking from sequential dual-polarization RADARSAT-2 images. *IEEE Transactions on Geoscience and Remote Sensing*, *52*(1), 121–136. https://doi.org/10.1109/TGRS.2012.2236845

Kwok, R. (2007). Baffin Bay ice drift and export: 2002–2007. *Geophysical Research Letters*, *34*(19), L19501. https://doi.org/10.1029/2007GL031204

Kwok, R., & Rothrock, D. A. (1999). Variability of Fram Strait ice flux and North Atlantic oscillation. *Journal of Geophysical Research*, *104*(C3), 5177–5189. https://doi.org/10.1029/1998JC900103

Kwok, R., Schweiger, A., Rothrock, D. A., Pang, S., & Kottmeier, C. (1998). Sea ice motion from satellite passive microwave imagery assessed with ERS SAR and buoy motions. *Journal of Geophysical Research*, *103*(C4), 8191–8214. https://doi.org/10.1029/97JC03334

Kwok, R., Toudal Pedersen, L., Gudmandsen, P., & Pang, S. S. (2010). Large sea ice outflow into the Nares Strait in 2007. *Geophysical Research Letters*, *37*(3), 2009GL041872. https://doi.org/10.1029/2009GL041872

Landy, J., & Dawson, G. (2022). Year-round Arctic sea ice thickness from CryoSat-2 Baseline-D Level1b observations 2010-2020 (version 1.0) [Dataset]. *NERC EDS UK Polar Data Centre*. https://doi.org/10.5285/d8c66670-57ad-44fc-8fef-942a46734ecb

Landy, J. C., Dawson, G. J., Tsamados, M., Bushuk, M., Stroeve, J. C., Howell, S. E. L., et al. (2022). A year-round satellite sea-ice thickness record from CryoSat-2. *Nature*, *609*(7927), 517–522. https://doi.org/10.1038/s41586-022-05058-5

Lavergne, T., Eastwood, S., Teffah, Z., Schyberg, H., & Breivik, L.-A. (2010). Sea ice motion from low-resolution satellite sensors: An alternative method and its validation in the Arctic. *Journal of Geophysical Research*, *115*(C10), 2009JC005958. https://doi.org/10.1029/2009JC005958

Liang, Y., Bi, H., Wang, Y., Huang, H., Zhang, Z., Huang, J., & Liu, Y. (2021). Role of extratropical wintertime cyclones in regulating the variations of Baffin Bay Sea Ice export. *JGR Atmospheres*, *126*(5), e2020JD033616. https://doi.org/10.1029/2020JD033616

Melling, H. (2002). Sea ice of the northern Canadian Arctic Archipelago. *Journal of Geophysical Research*, *107*(C11). https://doi.org/10.1029/2001JC001102

Moore, G. W. K. (2006). Reduction in seasonal sea ice concentration surrounding southern Baffin Island 1979–2004. *Geophysical Research Letters*, *33*(20), 2006GL027764. https://doi.org/10.1029/2006GL027764

Moore, G. W. K., Howell, S. E. L., Brady, M., Xu, X., & McNeil, K. (2021). Anomalous collapses of Nares Strait ice arches leads to enhanced export of Arctic sea ice. *Nature Communications*, *12*, 1. https://doi.org/10.1038/s41467-020-20314-w

Moore, G. W. K., & McNeil, K. (2018). The early collapse of the 2017 Lincoln Sea Ice arch in response to anomalous Sea Ice and wind forcing. *Geophysical Research Letters*, *45*(16), 8343–8351. https://doi.org/10.1029/2018GL078428

Ren, H., Shokr, M., Li, X., Zhang, Z., Hui, F., & Cheng, X. (2022). Estimation of Sea Ice production in the North Water polynya based on ice arch duration in winter during 2006–2019. *JGR Oceans*, *127*(10), e2022JC018764. https://doi.org/10.1029/2022JC018764

Smedsrud, L. H., Halvorsen, M. H., Stroeve, J. C., Zhang, R., & Kloster, K. (2017). Fram Strait sea ice export variability and September Arctic sea ice extent over the last 80 years. *The Cryosphere*, *11*(1), 65–79. https://doi.org/10.5194/tc-11-65-2017

Spreen, G., De Steur, L., Divine, D., Gerland, S., Hansen, E., & Kwok, R. (2020). Arctic Sea ice volume export through Fram Strait from 1992 to 2014. *JGR Oceans*, *125*(6), e2019JC016039. https://doi.org/10.1029/2019JC016039

Sumata, H., De Steur, L., Divine, D. V., Granskog, M. A., & Gerland, S. (2023). Regime shift in Arctic Ocean sea ice thickness. *Nature*, *615*(7952), 443–449. https://doi.org/10.1038/s41586-022-05686-x

Sumata, H., De Steur, L., Gerland, S., Divine, D. V., & Pavlova, O. (2022). Unprecedented decline of Arctic sea ice outflow in 2018. *Nature Communications*, *13*(1), 1747. https://doi.org/10.1038/s41467-022-29470-7

Tivy, A., Howell, S. E. L., Alt, B., McCourt, S., Chagnon, R., Crocker, G., et al. (2011). Trends and variability in summer sea ice cover in the Canadian Arctic based on the Canadian Ice Service Digital Archive, 1960–2008 and 1968–2008. *Journal of Geophysical Research*, *116*(C3), C03007. https://doi.org/10.1029/2009JC005855

Tschudi, M. A., Meier, W. N., & Stewart, J. S. (2020). An enhancement to sea ice motion and age products at the National Snow and Ice Data Center (NSIDC). *The Cryosphere*, *14*(5), 1519–1536. https://doi.org/10.5194/tc-14-1519-2020

Vincent, R. F. (2019). A study of the North Water polynya ice arch using four decades of satellite data. *Scientific Reports*, *9*(1), 20278. https://doi.org/10.1038/s41598-019-56780-6

Vincent, R. F. (2023). An assessment of the lancaster Sound polynya using satellite data 1979 to 2022. *Remote Sensing*, *15*(4), 954. https://doi.org/10.3390/rs15040954

Wilson, K. J., Barber, D. G., & King, D. J. (2001). Validation and production of RADARSAT-1 derived ice-motion maps in the North Water (NOW) polynya, January - December 1998. *Atmosphere-Ocean*, *39*(3), 257–278. https://doi.org/10.1080/07055900.2001.9649680